

---

## Supporting Information

**SI: Supporting Information for “FRETpredict: A Python Package for FRET efficiency predictions using Rotamer Libraries”.**

**S1 Text: Detailed description of the steps used to create new rotamer libraries.**

- 1. Generation of the conformational ensemble of the FRET probe.** We generated conformational ensembles of the FRET probes by performing replica exchange MD (REMD) simulations, using the force fields developed by Graen *et al.* [32] with some minor corrections [52]. From these trajectories, we here saved and analysed approximately 28,000 frames.
- 2. Selection of the peaks of the distributions of dihedral angles in the linkers.** We calculated the distributions of the dihedral angles in the linker using the conformational ensembles from REMD as input. Combinations of the dihedral angles corresponding to peaks in the dihedral distributions were combined to generate distinct probe conformers corresponding to C1 cluster centers.
- 3. First clustering step.** Trajectory frames are assigned to the C1 cluster centers of least-squares deviation of the dihedral angles.
- 4. Second clustering step.** Averages over the dihedral angles in the trajectory frames assigned to each cluster center are calculated to generate a new set of C2 center centers. As the C2 cluster centers do not necessarily represent physical conformations of the probe, they cannot not be directly used to build the rotamer library. Instead, the probe conformation with the minimum least-squares deviation from the C2 cluster center is chosen as the representative conformation of each center. Moreover, each C2 cluster center is assigned a weight equal to the number of conformations in the cluster (cluster population). When normalized over all clusters, this statistical weight approximates the Boltzmann probability of the representative conformation for a free dye in solution,  $p_i^{int}$ . These steps are sufficient for short linkers with few dihedral angles. However, for the longer linkers in many FRET probes, extra steps are needed to decrease the number of

rotamers while ensuring a good coverage of the conformational space. 613

**5. Filtering based on cluster populations.** In most cases, including all the C2 614  
cluster centers into the rotamer library (e.g., 8776 conformers for Lumiprobe 615  
Cy7.5 L1R) would defeat the purpose of using the RLA as its computational cost 616  
would be considerable, albeit much lower than for an MD simulation with explicit 617  
probes. Therefore, we implemented a weight-based cutoff to reduce the number of 618  
conformations in the library while maintaining a balanced coverage of the 619  
conformational space sampled by the probes. Namely, we filtered out C2 clusters 620  
with fewer than 10, 20, or 30 members, thus obtaining new sets of C3 clusters, 621  
which will be referred in this work as *large*, *medium*, and *small* rotamer libraries, 622  
respectively. Since filtering by the assigned weights skews the remaining weights 623  
from the underlying Boltzmann distribution, we implemented a third clustering 624  
step, in which the conformations previously belonging to a discarded C2 cluster 625  
are moved to the C3 cluster of minimum least-squares deviation, and the  $p_i^{int}$  626  
values are updated accordingly. 627

**6. Alignment and writing data to file.** The C3 cluster centers are aligned to the 628  
plane defined by the  $C\alpha$  atom and the C–N peptide bond. The resulting rotamer 629  
library is composed of a structure file (PDB format) and a trajectory file (DCD 630  
format) for the aligned FRET probe rotamers, and a text file containing the 631  
intrinsic Boltzmann weights of each rotamer state  $p_i^{int}$ . 632

---

## S2 Text Detailed description of the rotamer library placement and weighting steps.

**Rotamer library placement.** The first step in calculating FRET efficiencies is to place the FRET probes from the rotamer library at the protein site to be labeled, following the same procedure introduced in DEER-PREdict [29]. Briefly, the fluorophore library coordinates are translated and rotated based on the positions of the backbone  $C\alpha$ , amide N, and carbonyl C atoms. This results in a perfect overlap with the N and  $C\alpha$  coordinates of the protein backbone and an approximate alignment with the carbonyl C, which ensures that the  $C\alpha-C\beta$  vector of the probe has the correct orientation relative to the side chain of the labeled residue.

**Rotamer library weighting.** For each protein conformation, the overall probability of the  $i$ th rotamer of a probe is estimated by combining the intrinsic and the external Boltzmann probabilities of the inserted probe, independently from the other probe. The intrinsic probabilities,  $p_i^{in}$ , are obtained from the clustering procedure performed on the representative dihedral conformations of the free dye in solution and are related to the free energy of the rotamer,  $\epsilon_i^{int}$ , via Boltzmann inversion. Following the approach of Polyhach *et al.* [25], we account for the environment surrounding the FRET probe and calculate the probe-protein interaction energy,  $e_i^{ext}$ . This is achieved by summing up 12-6 Lennard-Jones pair-wise interaction energies between the heavy atoms of the probe and the surrounding protein within a 1-nm radius. The Lennard-Jones atomic radii ( $\sigma$ ) and potential-well depth ( $\epsilon$ ) parameters are obtained from the CHARMM36m force field [53]. The  $\sigma$  parameters can be scaled by a “forgive” factor which is set through the input parameter `sigma_scaling` and defaults to 0.5. This scaling compensates for inaccuracies in the placement of the bulky FRET probe, which tend to lead to clashes even for conformers with reasonably correct orientations of the probe with respect to the side chain of the labeled residue. The contribution of electrostatic interactions between charged probe and protein atoms is also taken into account using a dielectric constant of 78, and can be turned off by setting the `electrostatic` input parameter to `False`. Hence, the overall probability of the  $i$ th

rotamer state attached to the  $s$ th protein conformation is calculated as

662

$$p_{si} = p_i^{\text{int}} p_{si}^{\text{ext}} = p_i^{\text{int}} \frac{\exp(-e_{si}^{\text{ext}}/kT)}{Z}, \quad (10)$$

where  $Z = \sum_i p_i^{\text{int}} \exp(-e_{si}^{\text{ext}}/kT)$  is the steric partition function quantifying the fit of  
the rotamer in the embedding protein conformation. Low  $Z$  values result from large  
probe-protein interaction energies, suggesting tight placement of the probe due to either  
(i) misplacement of the rotamers or (ii) protein conformations incompatible with the  
presence of the FRET probe at the labeled site. Therefore, frames with  $Z < 0.05$  are  
discarded in the FRET efficiency calculation to preclude spurious conformers from  
contributing to the ensemble average, corresponding to a situation in which all of the  
rotamers have a positive steric energy. In FRETpredict, the default  $Z$  cutoff can be  
conveniently replaced by a user-provided value. This procedure could, in principle, be  
generalized to account for the effect of the probe on the protein free energy by weighting  
the protein conformations by the chromophore free energies  $-k_B T \ln(Z)$  in subsequent  
analysis, since the effect will differ by conformation even for those with  $Z$  above the  
cut-off.

663

664

665

666

667

668

669

670

671

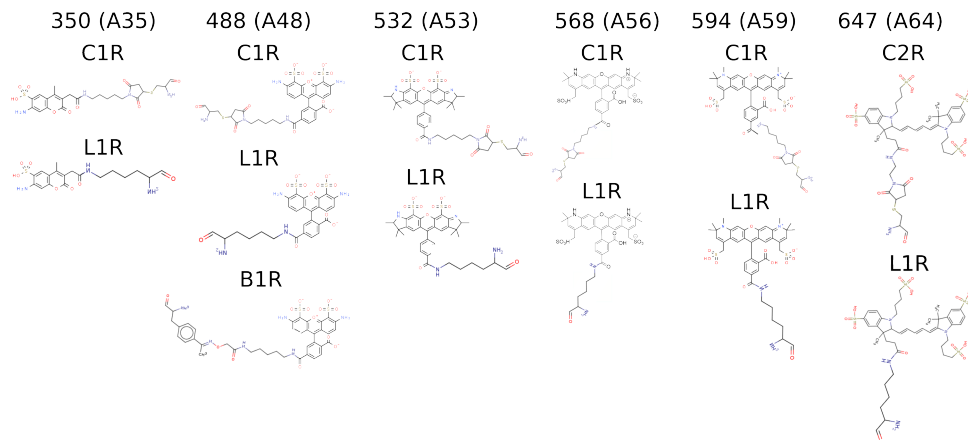
672

673

674

675

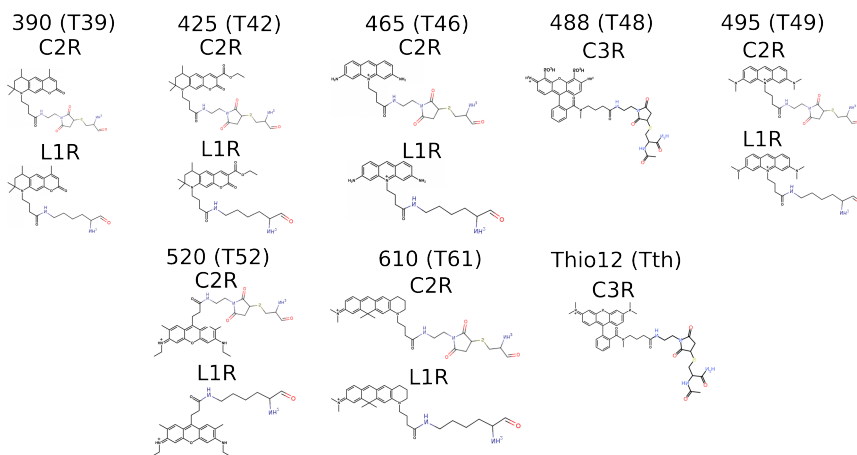
**S3 Figure: Structural formulae of the AlexaFluor probes.**



Structural formulae of the 13 AlexaFluor probes for which we generated rotamer libraries. Each column corresponds to a different fluorophore (acronym in parentheses). The names of the linkers are reported above each formula.

676

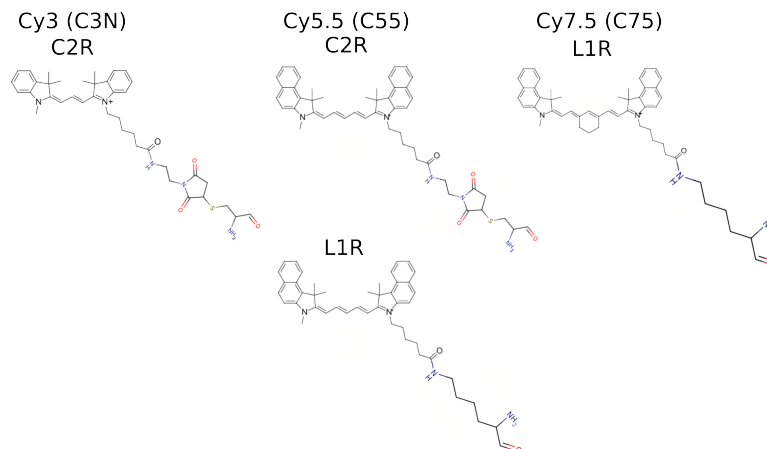
**S4 Figure: Structural formulae of the ATTO probes.**



Structural formulae of the 14 ATTO probes for which we generated rotamer libraries. Each column corresponds to a different fluorophore (acronym in parentheses). The names of the linkers are reported above each formula.

677

**S5 Figure: Structural formulae of the Lumiprobe probes.**

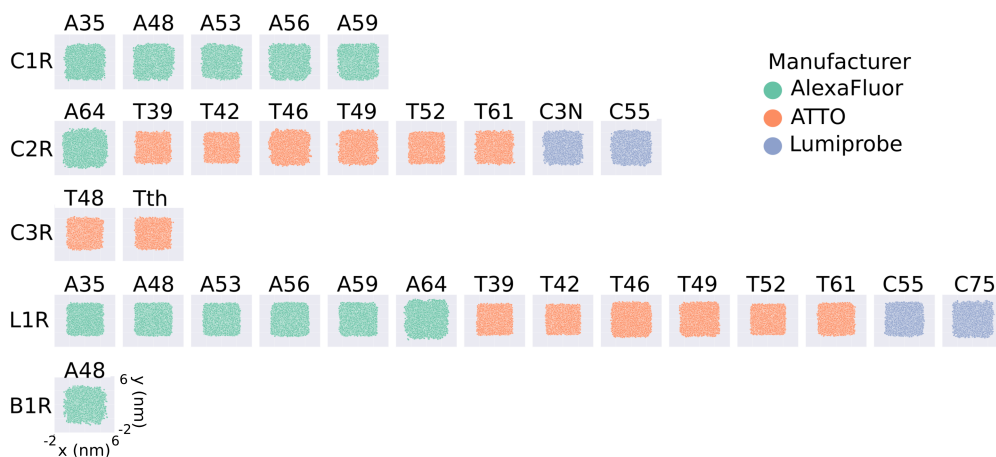


Structural formulae of the four Lumiprobe probes for which we generated rotamer libraries. Each column corresponds to a different fluorophore (acronym in parentheses). The names of the linkers are reported above each formula.

678

**S6 Figure: Scatter plot of Rotamer Libraries central atoms for unfiltered rotamer libraries (cutoff = 0).**

679

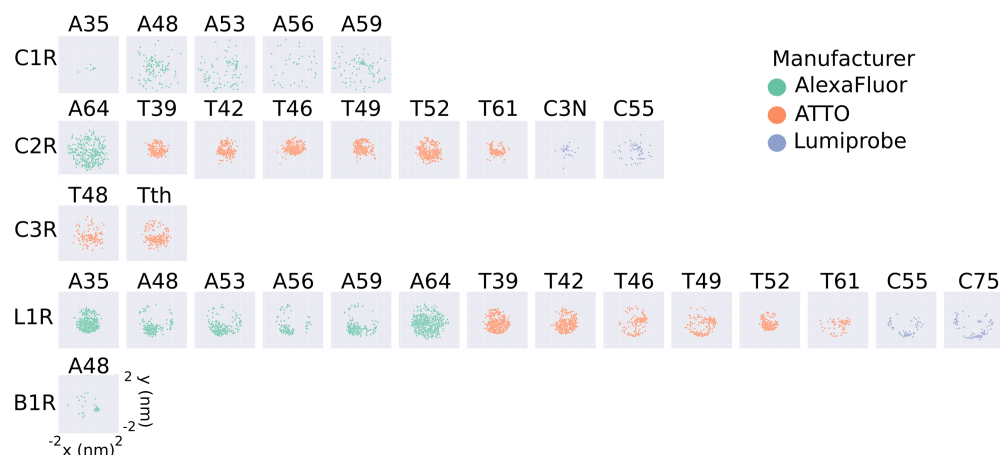


2D projections of the position of the fluorophore with respect to the C $\alpha$  atom for the unfiltered rotamer libraries generated in this work (C2 cluster centers). The projections are obtained as the  $x$  and  $y$  coordinates of the central atom of the fluorophore ( $O91$  for AlexaFluor,  $C7$  for ATTO, and  $C10$  for Lumiprobe), after placing the C $\alpha$  atom at the origin. Each plot represents a different FRET probe, divided into rows according to linker type (C1R, C2R, C3R, L1R, B1R, from top to bottom), and colored according to the manufacturer (green for AlexaFluor, orange for ATTO, and blue for Lumiprobe).

680

**S7 Figure: Scatter plot of medium-size rotamer libraries' central atoms (cutoff = 20).**

681



682

**S8 Figure: Scatter plot of small-size rotamer libraries central atoms (cutoff = 30).** 683

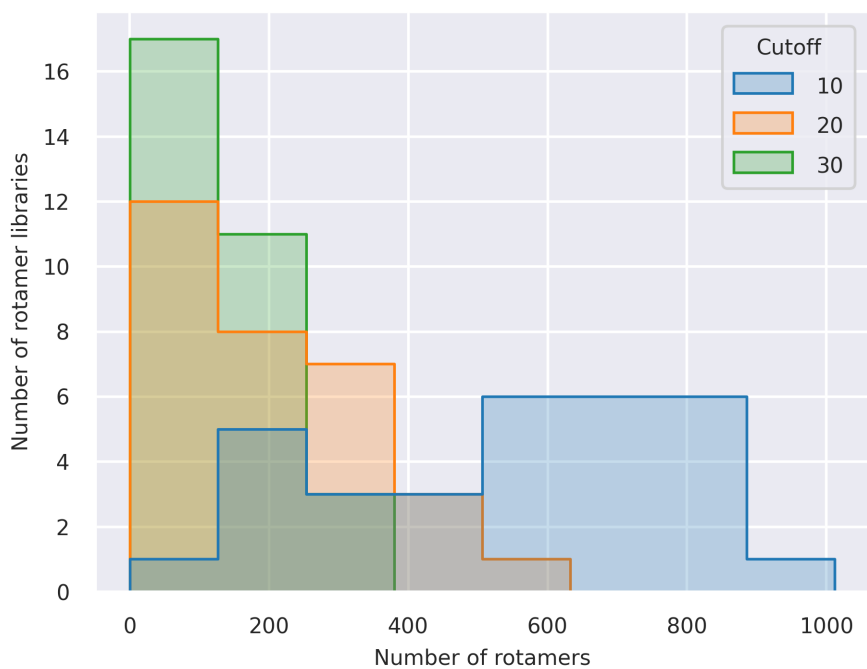


2D projections of the position of the fluorophore with respect to the  $C\alpha$  atom for the *small* rotamer libraries generated in this work. The projections are obtained as the  $x$  and  $y$  coordinates of the central atom of the fluorophore ( $O91$  for AlexaFluor,  $C7$  for ATTO, and  $C10$  for Lumiprobe), after placing the  $C\alpha$  atom at the origin. Each plot represents a different FRET probe, divided into rows according to linker type (C1R, C2R, C3R, L1R, B1R, from top to bottom), and colored according to the manufacturer (green for AlexaFluor, orange for ATTO, and blue for Lumiprobe).

684



**S9 Figure: Large, medium, and small rotamer libraries populations.**



Distribution of the number of conformers across all the *large* (blue), *medium* (orange), and *small* (green) rotamer libraries generated in this work.

**S10 Table: Computational times obtained using different cutoffs.**

	<i>small</i>	<i>medium</i>	<i>large</i>
Donor clusters	706	124	32
Acceptor clusters	574	106	38
Computation time	692 s	120 s	37 s

Computational times required to calculate FRET efficiency from a pp11 trajectory of 316 frames (Case study 1) using the *large* (cutoffs = 10), *medium* (cutoff = 20), and *small* rotamer libraries for AlexaFluor 488 - C1R and AlexaFluor 594 - C1R, on a laptop with AMD Ryzen 7 4800h processor with a Radeon graphics card. Compared to the *large* library, the *medium* library has significantly fewer cluster centers and it lowers the computational cost by a factor 6. Instead, choosing the *small* over the *medium* rotamer library results in a gain in computation time of around a factor of 3.

686

**S11 Table: FRETpredict  $E$  for Case study 1: pp11 (Fig 3).**

Polyproline 11 (pp11)			
Regime	<i>small</i>	<i>medium</i>	<i>large</i>
Static	0.732	0.745	0.743
Dynamic	0.876	0.886	0.881
Dynamic+	0.993	0.972	0.853
Average	0.917	0.912	0.89

FRET efficiencies calculated for pp11 using FRETpredict with different rotamer library sizes and three averaging regimes (Static, Dynamic, Dynamic+) as well as the average over those. The reference experimental value is 0.88 whereas the value obtained as the average over the three regimes from MD simulations with explicit FRET probes is 0.83.

687

**S12 Table: FRET efficiencies for Case study 2: ACTR (Fig 4).**

ACTR			
Residue pair (Regime)	[Urea] = 0 M	[Urea] = 2.5 M	[Urea] = 5 M
3-61 (Exp)	0.610	0.490	0.420
3-61 (Static)	0.602	0.374	0.319
3-61 (Dynamic)	0.698	0.451	0.382
3-61 (Dynamic+)	0.763	0.513	0.431
3-61 (Average)	0.688	0.446	0.377
3-75 (Exp)	0.470	0.380	0.340
3-75 (Static)	0.497	0.312	0.260
3-75 (Dynamic)	0.581	0.380	0.314
3-75 (Dynamic+)	0.639	0.437	0.360
3-75 (Average)	0.572	0.376	0.311
33-75 (Exp)	0.610	0.510	0.460
33-75 (Static)	0.476	0.474	0.450
33-75 (Dynamic)	0.574	0.567	0.539
33-75 (Dynamic+)	0.658	0.649	0.617
33-75 (Average)	0.570	0.563	0.535

ACTR FRET efficiencies calculated with FRETpredict for all residue pairs (3-61, 3-75, 33-75) at different urea concentrations (0 M, 2.5 M, and 5 M), for the *medium* rotamer library. The averaging regime is reported in parentheses.

**S13 Table: FRET efficiencies for Case study 3: Single structure proteins**

689

(Fig 5)

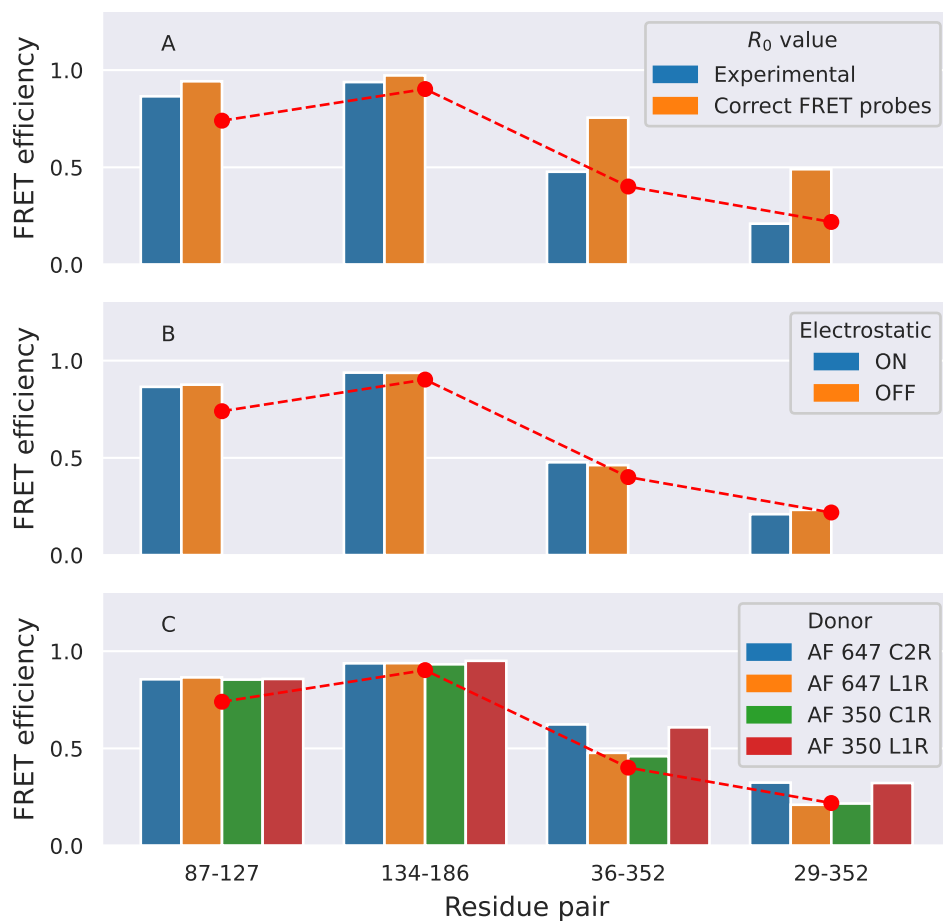
HiSiaP					
Residue pair (conformation)	Exp	Static	Dynamic	Dynamic+	Average
58-134 (open)	0.233	0.232	0.283	0.302	0.272
58-134 (closed)	0.321	0.284	0.364	0.379	0.342
55-175 (open)	0.765	0.554	0.723	0.890	0.722
55-175 (closed)	0.847	0.786	0.942	0.999	0.909
175-228 (open)	0.342	0.210	0.251	0.260	0.240
175-228 (closed)	0.300	0.311	0.388	0.410	0.370
112-175 (open)	0.437	0.260	0.318	0.343	0.307
112-175 (closed)	0.388	0.396	0.486	0.575	0.486
SBD2					
Residue pair (conformation)	Exp	Static	Dynamic	Dynamic+	Average
319-392 (open)	0.408	0.174	0.197	0.215	0.195
319-392 (closed)	0.661	0.614	0.792	0.920	0.775
369-451 (open)	0.275	0.270	0.296	0.304	0.290
369-451 (closed)	0.469	0.477	0.587	0.627	0.564
MaLE					
Residue pair (conformation)	Exp	Static	Dynamic	Dynamic+	Average
87-127 (open)	0.740	0.749	0.887	0.959	0.865
87-127 (closed)	0.577	0.515	0.666	0.771	0.651
134-186 (open)	0.903	0.857	0.964	0.994	0.938
134-186 (closed)	0.913	0.819	0.949	0.989	0.919
36-352 (open)	0.401	0.411	0.491	0.530	0.477
36-352 (closed)	0.672	0.548	0.692	0.825	0.688
29-352 (open)	0.219	0.177	0.217	0.237	0.210
29-352 (closed)	0.359	0.321	0.415	0.486	0.407

FRET efficiencies calculated with FRETpredict for the open and closed conformations of all the single-structure proteins (HiSiaP, SBD2, and MaLE), for the *large* rotamer library. Every row corresponds to a labeled residue pair, with the protein conformation reported in parentheses. Every column corresponds to an averaging regime or to the experimental value for the specific residue pair and protein conformation.

690

**S14 Figure: Physicochemical parameters affecting FRETpredict calculations.**

691



Effects of different physicochemical parameters on FRETpredict calculation ( $R_0$ , probe steric bulk, and electrostatics, in panels A, B, and C, respectively). Calculations were performed on the open structure of MalE with the *large* rotamer library. Reported FRET efficiencies in all panels correspond to the average over the different regimes. In panel A, the  $R_0$  value is changed from the experimental value of 5.1 nm (blue bars) to the actual  $R_0$  of the two FRET probes used in the calculations (AlexaFluor 647 - AlexaFluor 647), i.e., 6.50 nm (orange bars). In panel B, the FRET efficiency was computed by turning electrostatic interactions on (blue bars) or off (orange bars) in the calculation of probe-protein energies. In panel C, the donor FRET probe is AlexaFluor 647 C2R (blue bars), AlexaFluor 647 L1R (orange bars), AlexaFluor 350 C1R (green bars), and AlexaFluor 350 L1R (red bars).

692